Constructing an Equation of State for a Diatomic Gas

Noah Blair and Dr. Matthew Semak

Department of Physics and Astronomy
University of Northern Colorado

Abstract

In the interest of better understanding systems of interacting particles in equilibrium, the grand canonical partition function for a diatomic gas is computed using the Lennard-Jones potential to model molecular interactions. This was used to find a correction to the ideal gas law by calculating the second virial coefficient. This allowed us to construct an equation of state that was checked by referring to empirical measurements of the pressure, temperature, and volume of diatomic oxygen as well as a Monte Carlo simulation of gases.

Introduction

The fundamental assumptions of an ideal gas are that the molecules do not contain any internal structure (rotational and vibrational states), and that there are no intermolecular interactions. The compressibility, Z, quantifies how the behavior of a real gas reflects that of an ideal gas. It is often expressed in the following way:

$$Z = PV/Nk_BT = PV\beta/N,$$

where P is the pressure, V is the volume, N is the number of particles, k_B is the Boltzmann constant, and T is the temperature. For an ideal gas, Z=1. For monatomic gases, this is a valid approximation for the dynamics near $300\ K$. However, for diatomic molecules, there are energy states due to rotations of the molecule and vibrations, as well as short range molecular interactions. Examining empirical data from NIST [1], it was found that the compressibility of diatomic oxygen is within 0.1 of that for an ideal gas for temperatures ranging from $100\ K \rightarrow 1000\ K$. Given this, we may write the compressibility in the following way [2]:

$$Z = 1 - \frac{N}{V}B(T),$$

where $B(T)$ is known as the second virial coefficient and models how the dynamics differ from those for an ideal gas. We used the Lennard-Jones (6-12) potential (Figure 1) to model the intermolecular interactions that occur. This potential both accurately reflects experimental measurements for forces molecules exert on each other, and is more mathematically convenient to use than other commonly used intermolecular potentials.

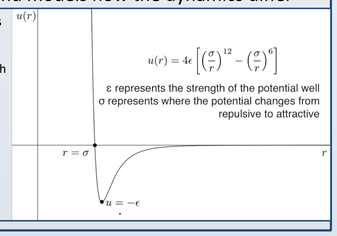

Figure (1) shows the Lennard-Jones potential. This models both repulsive and attractive interactions.

Grand Canonical Partition Function and Virial Coefficients

The grand canonical partition function, Ξ, allows us to calculate the probability of a system being in a given state and allows us to compute dynamical variables, such as the pressure and compressibility [3]:

$$\mathrm{Z} = \ln \Xi\ /N\ .$$

The partition function for our system is given by [3]:

$$\ln \Xi = \sum_{n=1}^{\infty} \frac{V\Lambda^n}{\lambda_T^{3n}} e^{n\beta\mu} b_n(T)\ ,$$

where Λ and λ_T are the contributions due to the internal rotational and vibrational states [2] and the kinetic energy of the system, respectively. Also, μ is the chemical potential of the substance. The set of functions $\{b_n(T)\}$ are given by:

$$b_n(T) = \frac{1}{(n!)V}\int d^3r_1 \cdots d^3r_n U_n(r_1, \cdots, r_n)\ ,$$

where $U_n(r_1, \cdots, r_n)$ are the cluster functions that contain the various intermolecular interaction terms. These functions can be used to generate our virial coefficients. A single particle cannot interact with itself, which gives $b_1(T) = 1$. $b_2(T)$, which relates to the interaction between two particles, is our second virial coefficient. This will take the following form after non-trivial manipulation [2,3]:

$$B(T) = -b_2(T) = -2\pi\int_0^{\infty} r^2\left(e^{-\beta u(r)} - 1\right)dr,$$

where u(r) in this case is the Lennard-Jones potential. Therefore, our compressibility will be:

$$\mathrm{Z} = \frac{PV}{Nk_BT} = 1 - 2\pi\frac{N}{V}\int_0^{\infty} r^2\left(e^{-\beta u(r)} - 1\right)dr.$$

The Second Virial Coefficient

After manipulation of the expression for $b_2(T)$, the second virial coefficient was found to be:

$$B(T) = \frac{-\pi\sigma^3}{6}\sum_{n=1}^{\infty}\frac{2^{n+\frac{1}{2}}}{n!}\Gamma\left(\frac{2n-1}{4}\right)\left(\frac{\varepsilon}{k_BT}\right)^{\frac{2n-1}{4}},$$

where $\Gamma\ (x)$ is known as the gamma function. We find that this series converges rapidly after the first ten terms. The partition function will now be:

$$\Xi \approx \exp\left(\frac{V\Lambda}{\lambda_T^3}e^{\beta\mu} + \frac{\pi\sigma^3}{6}\frac{V\Lambda^2}{\lambda_T^6}e^{2\beta\mu}\sum_{n=1}^{\infty}\frac{2^{n+\frac{1}{2}}}{n!}\Gamma\left(\frac{2n-1}{4}\right)\left(\frac{\varepsilon}{k_BT}\right)^{\frac{2n-1}{4}}\right).$$

This allows us to get the internal energy [2]:

$$E = -\partial \ln \Xi/\partial\beta,$$

and the compressibility:

$$Z = 1 - \frac{N}{V}\frac{\pi\sigma^3}{6}\sum_{n=1}^{\infty}\frac{2^{n+\frac{1}{2}}}{n!}\Gamma\left(\frac{2n-1}{4}\right)\left(\frac{\varepsilon}{k_BT}\right)^{\frac{2n-1}{4}}.$$

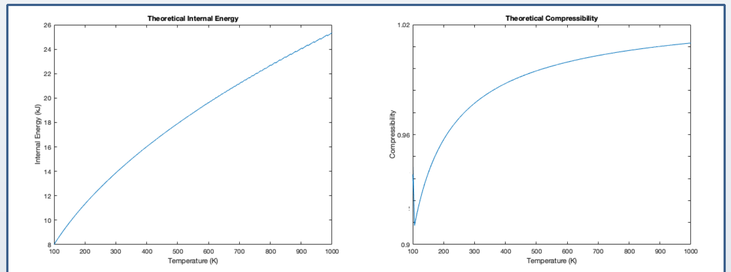

Figure (2) shows the theoretical internal energy versus temperature (left) and the compressibility vs temperature (right).

We see (Figure 2) that the internal energy increases less rapidly than would be expected in comparison to experimental results (Figure 4).

Monte Carlo Simulation of the Lennard-Jones Gas

In addition to theoretical calculations and empirical data, a Monte Carlo simulation [5] was used to analyze the dynamics of a gas as it approaches equilibrium with interactions described by the Lennard-Jones potential. During each iteration of the algorithm, the particles are displaced in a manner following Boltzmann statistics for a given temperature [6]. After a given displacement, if the system energy is not optimized, the step is not accepted. After this has been performed for a random sampling of particles, the iteration repeats. The algorithm allows for 100 iterations for the system to reach equilibrium. This process is repeated for system temperatures corresponding to $100\ K \rightarrow 1000\ K$ in steps of from $16\ K$. At equilibrium, the pressure and energy are computed.

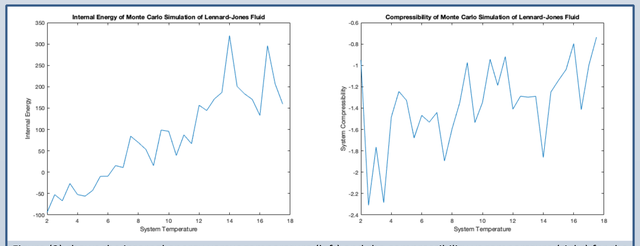

Figure (3) shows the internal energy versus temperature (left) and the compressibility vs temperature (right) for the simulation. Temperatures are scaled for the simulation.

The simulation is currently allowing improbable displacements, likely due to an error in the random number generator (Figure 3). We are still in the process of modifying the algorithm to produce reasonable results for the energy and compressibility of the gas.

Empirical Data

We obtained measurements of the pressure, internal energy, temperature, and volume of diatomic oxygen for isochoric processes (constant volume) for temperatures ranging from $100\ K \rightarrow 1000\ K$ (Figure 4). This allows us to compare our theoretical calculations to empirical measurements. Diatomic oxygen was chosen due to its low freezing point.

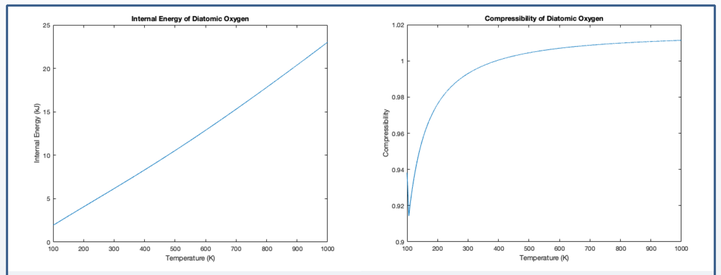

Figure (4) shows the internal energy versus temperature (left) and the compressibility vs temperature (right) for diatomic oxygen.

Results

The theoretical calculations of the compressibility seem to match the experimental results; minor deviations no greater than 0.01 at the maximum are present (Figure 5). At higher temperatures these deviations are more obvious. Inclusion of a third virial coefficient may remedy the deviations. A curious phenomenon that occurs in both the theoretical and experimental data is the drop in the compressibility near 100 K. This can possibly be explained by oxygen occupying liquid states at lower temperatures, but the full explanation for this will be explored in further projects. The discrepancy in the energy profiles between experiment and theory is also not completely understood at this point. We anticipate that it is related to rotational and vibrational states providing negligible energy at lower temperatures.

With regards to the Monte Carlo simulation, we plan to modify how the energy and pressure are computed to improve accuracy. For future research, we plan to investigate how perturbations to the Lennard-Jones potential affect the dynamics of a gas, as well as behavior in the temperature range near the liquid-gas phase transition.

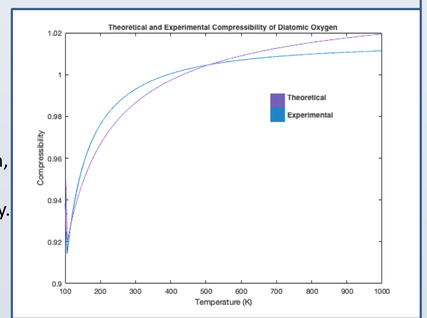

Figure (5) shows the theoretical and experimental compressibility of diatomic oxygen.

Acknowledgements

We would like to thank the entire Department of Physics and Astronomy. We are particularly grateful to Dr. Walch, Dr. Chaloupka, and Dr. Galovich for their support and advice through the project. We would also like to thank Dr. Weinrich (UNCO's Department of Chemistry and Biochemistry) and Richard Miller (UNCO Department of Physics and Astronomy Graduate) for input on chemical data.

References

[1] - P.J. Linstrom and W.G. Mallard, Eds., NIST Chemistry WebBook, NIST Standard Reference Database Number 69, National Institute of Standards and Technology, Gaithersburg MD, 20899, https://doi.org/10.18434/T4D303, (retrieved January 26, 2019)

[2] - Schroeder, D. V. (2005). *An Introduction to Thermal Physics*. San Francisco, CA: Addison Wesley Longman.

[3] - Reichl, L. E. (1998). *A Modern Course in Statistical Physics* (2nd ed.). New York, NY: Wiley.

[4] - Bouanich, J. (1992). Site-site Lennard-Jones potential parameters for N2, O2, H2, CO and CO2. *Journal of Quantitative Spectroscopy and Radiative Transfer, 47*(4), 243-250. doi:10.1016/0022-4073(92)90142-q

[5] - Benjamini, A. (2012, August 20). Understanding Molecular Simulations. Retrieved February 18, 2019, from http://www.cchem.berkeley.edu/chem195/

[6] - Metropolis, N., Rosenbluth, A. W., Rosenbluth, M. N., Teller, A. H., & Teller, E. (1953). Equation of state calculations by fast computing machines. *Journal of Chemical Physics, 21*(6). doi:10.2172/4390578

[7] - Abrams, C. (2314, March 3). Case Study 4 (F&S Case Study 1): Equation of State of the Lennard-Jones Fluid. Retrieved February 23, 2019, from http://www.pages.drexel.edu/~cfa22/msim/node19.html